Facile Template Synthesis of Ordered Mesoporous Carbon with Polypyrrole as Carbon Precursor

Chia-Min Yang,[†,‡] Claudia Weidenthaler,[†] Bernd Spliethoff,[†] Mamatha Mayanna,[†] and Ferdi Schüth*[,†]

Max-Planck-Institut für Kohlenforschung, Kaiser-Wilhelm-Platz 1, D-45470 Mülheim an der Ruhr, Germany, and Department of Chemistry, National Tsing Hua University, Hsinchu 30013, Taiwan

Received May 26, 2004. Revised Manuscript Received August 26, 2004

A new and facile synthetic route of ordered mesoporous carbon with polypyrrole as carbon precursor has been developed. The mesoporous silica host is first impregnated with ferric chloride, which serves as the oxidant for the vapor-phase oxidative polymerization of pyrrole vapor at room temperature. Such a stoichiometric reaction provides a rational control of loading with polypyrrole and also determines the amount of carbon after subsequent pyrolysis in the host silica. Ordered mesoporous carbon is obtained after the dissolution of silica and iron species. The materials thus prepared have ordered structure, large surface area, and pore volume. They are ordered on the mesoscopic scale and show some graphitic order on the atomic scale.

Introduction

Nanostructured carbon materials attract much attention due to their uses as adsorbents, catalyst supports, and electrode materials.[1−4] Recently, a new class of nanostructured carbons, i.e., ordered mesoporous carbons (OMCs), have been synthesized using ordered mesoporous silica as a template.[1c,2c,3c−d,5−10] Compared to carbon materials with disordered pore structures, OMCs allow rational control over their pore diameters and arrangements, which is crucial for applications requiring narrow pore size distribution and pore accessibility.

The preparation of OMCs generally involves incorporation of a carbon precursor (such as sucrose, furfuryl alcohol, acetylene, acenaphthene, or phenol resin) through either a solution-phase or a vapor-phase reaction to mesoporous silica hosts in the presence of a catalyst, followed by the pyrolysis of the carbon precursor. Another synthetic route by catalytic chemical vapor deposition has also been described.[8] The OMC replicas prepared by different methods usually bear different morphologies (e.g., rodlike or tube-like structure) and properties,[9] which largely depend on the choice of the carbon precursor as well as the pyrolysis condition. However, there is still a high demand to explore new methods to prepare OMCs with specific morphology and properties.

Here we report an alternative route for template synthesis of OMC using polypyrrole (Ppy) as carbon precursor and ferric chloride ($FeCl_3$) as the oxidant. Ppy is a conducting polymer, which has been shown to be a good precursor to prepare graphitic carbon nanostructures.[11] The pyrrole monomer has relatively high vapor pressure at room temperature, allowing a facile vapor-phase oxidative polymerization of pyrrole in the $FeCl_3$-impregnated mesoporous silica. In addition, the polymerization reaction is stoichiometric between pyrrole and $FeCl_3$, hence the loading of Ppy can be rationally controlled by the amount of impregnated $FeCl_3$.

* To whom correspondence should be addressed. E-mail: schueth@mpi-muelheim.mpg.de.
† Max-Planck-Institut für Kohlenforschung.
‡ National Tsing Hua University.

(1) (a) Suda, H.; Haraya, K. *J. Phys. Chem. B* **1997**, *101*, 3988. (b) Suda, H.; Haraya, K. *Chem. Commun.* **1997**, 93. (c) Ohkubo, T.; Miyawaki, J.; Kaneko, K.; Ryoo, R.; Seaton, N. A. *J. Phys. Chem. B* **2002**, *106*, 6523.
(2) (a) Foley, H. C. *Microporous Mater.* **1995**, *4*, 407. (b) Rodriquez-Reinoso, F. *Carbon* **1998**, *36*, 159. (c) Ahn, W. S.; Min, K. I.; Chung, Y. M.; Rhee, J. K.; Joo, S. H.; Ryoo, R. *Stud. Surf. Sci. Catal.* **2001**, *135*, 313.
(3) (a) Flandrois, S.; Simon, B. *Carbon* **1999**, *37*, 165. (b) Lee, J.; Yoon, S.; Oh, S. M.; Shin, C. H.; Hyeon, T. *Adv. Mater.* **2000**, *12*, 359. (c) Yoon, S. B.; Kim, J. Y.; Yu, J. S. *Chem. Commun.* **2001**, 2177. (d) Joo, S. H.; Choi, S. J.; Oh, I.; Kwak, J.; Liu, Z.; Terasaki, O.; Ryoo, R. *Nature* **2001**, *412*, 169.
(4) (a) Liu, C.; Fan, Y. Y.; Liu, M.; Cong, H. T.; Cheng, H. M.; Dresselhaus, M. S. *Science* **1999**, *286*, 1127. (b) Schlapbach, L.; Züttel, A. *Nature* **2001**, *414*, 353. (c) Hirscher, M.; Becher, M.; Haluska, M.; von Zeppelin, F.; Chen, X.; Dettlaff-Weglikowska, U.; Roth, S. *J. Alloys Compd.* **2003**, *356−357*, 433. (d) Smith, M. R.; Bittner, E. W.; Shi, W.; Johnson, J. K.; Bockrath, B. C. *J. Phys. Chem. B* **2003**, *107*, 3752. (e) Hou, P. X.; Xu, S. T.; Ying, Z.; Yang, Q. H.; Liu, C.; Cheng, H. M. *Carbon* **2003**, *41*, 2471.
(5) (a) Ryoo, R.; Joo, S. H.; Jun, S. *J. Phys. Chem. B* **1999**, *103*, 7743. (b) Jun, S.; Joo, S. H.; Ryoo, R.; Kruk, M.; Jaroniec, M.; Liu, Z.; Ohsuna, T.; Terasaki, O. *J. Am. Chem. Soc.* **2000**, *122*, 10712. (c) Ryoo, R.; Joo, S. H.; Kruk, M.; Jaroniec, M. *Adv. Mater.* **2001**, *13*, 677. (d) Lee, J. S.; Joo, S. H.; Ryoo, R. *J. Am. Chem. Soc.* **2002**, *124*, 1156. (e) Solovyov, L. A.; Shmakov, A. N.; Zaikovskii, V. I.; Joo, S. H.; Ryoo, R. *Carbon* **2002**, *40*, 2477. (f) Kaneda, M.; Tsubakiyama, T.; Carlsson, A.; Sakamoto, Y.; Ohsuna, T.; Terasaki, O.; Joo, S. H.; Ryoo, R. *J. Phys. Chem. B* **2002**, *106*, 1256. (g) Kruk, M.; Jaroniec, M.; Kim, T. W.; Ryoo, R. *Chem. Mater.* **2003**, *15*, 2815.
(6) (a) Kim, S. S.; Pinnavaia, T. J. *Chem. Commun.* **2001**, 2418. (b) Yu, C.; Fan, J.; Tian, B.; Zhao, D. Stucky, G. D. *Adv. Mater.* **2002**, *14*, 1742.
(7) (a) Lee, J.; Yoon, S.; Hyeon, T.; Oh, S. M.; Kim, K. B. *Chem. Commun.* **1999**, 2177. (b) Lee, J.; Sohn, K.; Hyeon, T. *J. Am. Chem. Soc.* **2001**, *123*, 5146. (c) Yoon, S. B.; Kim, J. Y.; Yu, J. S. *Chem. Commun.* **2001**, 559.
(8) Zhang, W. H.; Liang, C.; Sun, H.; Shen, Z.; Guan, Y.; Ying, P.; Li, C. *Adv. Mater.* **2002**, *14*, 1776.
(9) Kim, T. W.; Park, I. S.; Ryoo, R. *Angew. Chem., Int. Ed.* **2003**, *42*, 4375.
(10) Lu, A. H.; Schmidt, W.; Spliethoff, B.; Schüth, F. *Adv. Mater.* **2003**, *15*, 1602.
(11) Jang, J.; Oh, J. H.; Stucky, G. D. *Angew. Chem., Int. Ed.* **2002**, *41*, 4016.

10.1021/cm049164v CCC: $30.25
Published on Web 12/04/2004

After pyrolysis and dissolution of host silica and iron species, OMC with high surface area, large pore volume, and some characteristic features of graphite can be prepared. In addition, this method may also be applied to prepare carbon replicas of mesoporous silica with fiber or film morphologies, for which other synthetic routes are difficult to realize.

Experimental Section

Synthesis. Mesoporous silica SBA-15 was prepared by adding tetraethoxysilane (TEOS) into the hydrochloric acid solution of triblock copolymer P123.[11] The molar composition was 1:5.9:193: 0.017 TEOS/HCl/H_2O/P123. The mixture was stirred at 40 °C for 20 h, followed by aging at 90 °C for 24 h. The solid was filtered and dried, and was calcined at 540 °C. The synthesis of mesoporous silica MCM-48 was based on a reported procedure using sodium silicate as silica source and a mixture of cetyltrimethylammonium bromide (CTAB) and Brij 30 as structure directing agent.[15c] The as-prepared high-quality MCM-48 was also calcined at 540 °C.

For the preparation of the OMC replica, 1.0 g of host silica (SBA-15 or MCM-48) was first impregnated with 0.2−2.5 g of $FeCl_3$ dissolved in 1.0−1.5 mL of 1.0 M HCl aqueous solution. The yellowish sample was dried at 90 °C for 2 h, and was then treated with saturated pyrrole vapor at room temperature for another 2 h. *Caution: Pyrrole vapor is toxic. Perform the experiments in the hood and prevent any contact of the vapor with skins and eyes*. After the reaction, the resulting dry black powder was collected. The pyrolysis of Ppy was performed in an argon flow at 850 °C for 5 h with a temperature ramp of 5 K min^{-1}. The host silica and the iron species were dissolved subsequently by diluted HF and HCl solutions.

Characterization. XRD patterns were obtained on a Stoe STADI P diffractometer in the reflection mode using Cu Kα radiation. Nitrogen sorption isotherms were measured at 77 K using a Micromeritics ASAP 2010 instrument. The pore diameter and the pore size distribution were calculated from the desorption branch using the Barrett−Joyner−Halenda (BJH) method. The loadings of Ppy and pyrolyzed carbon in the composites were determined from the weight loss curves measured under air atmosphere on a TG/DTA instrument (Netzsch STA 449 C) with a heating rate of 10 K min^{-1}. The TEM images were obtained with a Hitachi HF2000 electron microscope. XPS measurements were performed with a Kratos HSi spectrometer with a hemispherical analyzer. The monochromatized Al Kα X-ray source (E = 1486.6 eV) was operated at 15 kV and 20 mA. For the narrow scans, an analyzer pass energy of 40 eV was applied. The hybrid mode was used as lense mode. The base pressure in the analysis chamber was 4×10^{-9} Torr. To account for charging effects, all spectra have been referred to Si 2p at 103.3 eV.

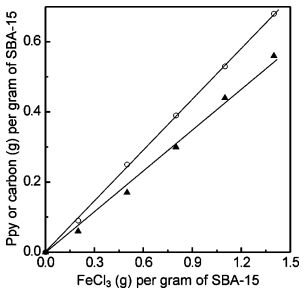

Figure 1. Dependence of the loadings of Ppy (○) and carbon after pyrolysis (▲) on the amount of impregnated $FeCl_3$ in SBA-15.

Results and Discussion

The oxidative polymerization of pyrrole and $FeCl_3$ is stoichiometric. Mesoporous silica SBA-15 was first used as the template, and Figure 1 shows the dependence of Ppy loading in SBA-15 on the $FeCl_3$ amount. A nearly linear relationship between them was found, and the molar ratio of pyrrole monomer to $FeCl_3$ was about 1.2. The value is very close to 1, which is the expected value for the stoichiometric reaction. The slight deviation from the stoichiometry may be due to iron species inaccessible to the pyrrole vapor and some contribution to the oxidation reaction by oxygen from the atmosphere. After pyrolysis in slow argon flow, about 75−80 wt % of carbon species remained in the composite. The relatively high amount of remaining carbon may be due to different pyrolysis behavior of Ppy in the confined space under the pyrolysis condition. In addition, the iron species present in the sample may catalyze the graphitization of carbon and reduce its weight loss during pyrolysis.[11] The amount of pyrolyzed carbon also shows a roughly linear relationship with $FeCl_3$ amount, which provides the basis for a rational control of the carbon loading in the silica template.

Pure carbon materials could be obtained after dissolving the host silica and iron. It was found that the amount of pyrolyzed carbon is crucial for replicating the ordered structure of the SBA-15 template. A minimum amount of 0.30 g per g of SBA-15, corresponding to an impregnation amount of $FeCl_3$ of about 0.8 g per g of SBA-15, was necessary to obtain a hexagonally structured carbon replica. Smaller amounts of pyrolyzed carbon were found to be insufficient to produce a replica structure. However, if the impregnated $FeCl_3$ exceeded 2.0 g per g of SBA-15, significant amounts of Ppy (and therefore pyrolyzed carbon) was deposited on the outer surface of the host silica. This may also take place at low loading of $FeCl_3$, but the fraction of $FeCl_3$ deposited on the external surface is small, since the carbons were almost exclusively well structured which is not expected for external deposition.

The OMC replica prepared from the sample impregnated with 1.0 g of $FeCl_3$ per gram of SBA-15 was further characterized in more detail. The comparison of the XRD patterns of the host SBA-15 and its OMC replica is shown in Figure 2a. The XRD pattern of the replica is well-resolved

(12) (a) Zhao, D.; Feng, J.; Huo, Q.; Melosh, N.; Fredrickson, G. H.; Chmelka, B. F.; Stucky, G. D. *Science* **1998**, *279*, 548. (b) Zhao, D.; Huo, Q.; Feng, J.; Chmelka, B. F.; Stucky, G. D. *J. Am. Chem. Soc.* **1998**, *120*, 6024. (c) Galarneau, A.; Cambon, H.; Di Renzo, F.; Ryoo, R.; Choi, M.; Fajula, F. *New J. Chem.* **2003**, *27*, 73.

(13) (a) Malitesta, C., Morea, G., Sabbatini, L., Zambonin, P. G., Eds. *Surface Characterization of Advanced Polymers*; VCH: Weinheim, 1993; p 181. (b) Malitesta, C.; Losito, I.; Sabbatini, L.; Zambonin, P. G. *J. Electron Spectrosc. Relat. Phenom.* **1995**, *76*, 629. (c) Raymundo-Piñero, E.; Cazorla-Amorós, D.; Linares-Solano, A.; Find, J.; Wild, U.; Schlögl, R. *Carbon* **2002**, *40*, 597. (d) Diaz, J.; Paolicelli, G.; Ferrer, S.; Comin, F. *Phys. Rev. B* **1996**, *54*, 8064.

(14) (a) Darmstadt, H.; Roy, C.; Kaliaguine, S.; Joo, S. H.; Ryoo, R. *Microporous Mesoporous Mater.* **2003**, *60*, 139. (b) Darmstadt, H.; Roy, C.; Kaliaguine, S.; Kim, T. W.; Ryoo, R. *Chem. Mater.* **2003**, *15*, 3300.

(15) (a) Kresge, C. T.; Leonowicz, M. E.; Roth, W. J.; Vartuli, J. C.; Beck, J. S. *Nature* **1992**, 359, 710. (b) Beck, J. S.; Vartuli, J. C.; Roth, W. J.; Leonowicz, M. E.; Kresge, C. T.; Schmitt, K. D.; Chu, C. T.-W.; Olson, D. H.; Sheppard, E. W.; McCullen, S. B.; Higgins, J. B.; Schlenker, J. L. *J. Am. Chem. Soc.* **1992**, *114*, 10834. (c) Ryoo, R.; Joo, S. H.; Kim, J. M. *J. Phys. Chem. B* **1999**, *103*, 7435.

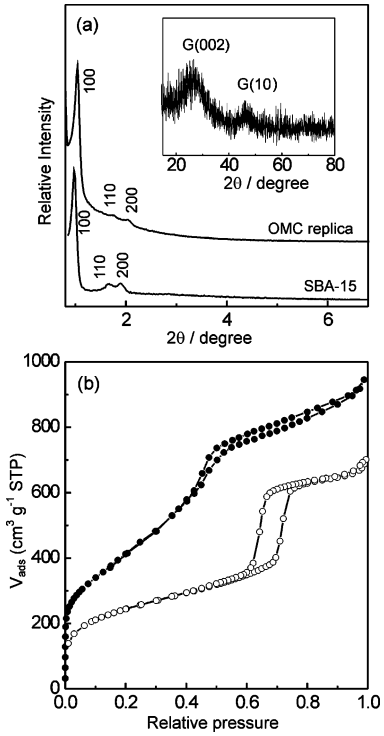

Figure 2. (a) XRD patterns of SBA-15 and the OMC replica. The inset shows the wide-angle XRD pattern of the OMC replica. (b) Nitrogen sorption isotherms of SBA-15 (○) and the OMC replica (●).

and the reflections can be assigned to (100), (110), and (200) reflections of the 2-D hexagonal *p*6*mm* space group, indicating a retention of the ordered structure of its parent SBA-15 host. This indicates that while the amount of pyrolyzed carbon deposited in both the mesopores and complementary mesopores/micropores of SBA-15[12c] was not high enough to fill the pores completely, it was sufficient to prevent the collapse of the mesostructured carbon after dissolving the host silica. The cell parameter of the OMC replica (9.8 nm) is smaller than that of the host SBA-15 (10.5 nm), which may result from the shrinkage of the carbon/silica composite material during pyrolysis and dissolution of host silica.

Figure 2b shows the nitrogen sorption isotherms of SBA-15 and its OMC replica. The sharp step with a hysteresis loop for the isotherm of host SBA-15 indicates a narrow pore size distribution and a uniform mesopore diameter of 6.7 nm. On the other hand, the isotherm for the OMC replica shows a step at relative pressure between 0.43 and 0.50, suggesting a pore-size distribution centered at 4.2 nm. This value is in agreement with the wall thickness of the host SBA-15.[5b] In addition to the void space from the dissolved silica, the porosity of OMC replica is also generated by the insufficient filling of Ppy in the host silica and the dissolution of iron species by HCl. Therefore, the sorption isotherms of the OMC materials do not have sharp steps corresponding to the replica structure of the host silica. However, it is difficult to distinguish all these contributions in a single sorption isotherm. The isotherm of the OMC material also allows calculation of a high BET surface area of 1560 m^2g^{-1} and large total pore volume of 1.4 cm^3g^{-1}. The total pore volume is primarily related to the volume of the ordered pores with minor contribution from micropores and possibly also from secondary mesopores. The hysteresis does not close at high relative pressure, which might be a result of interparticle textural pores in the mesoporous carbon material.

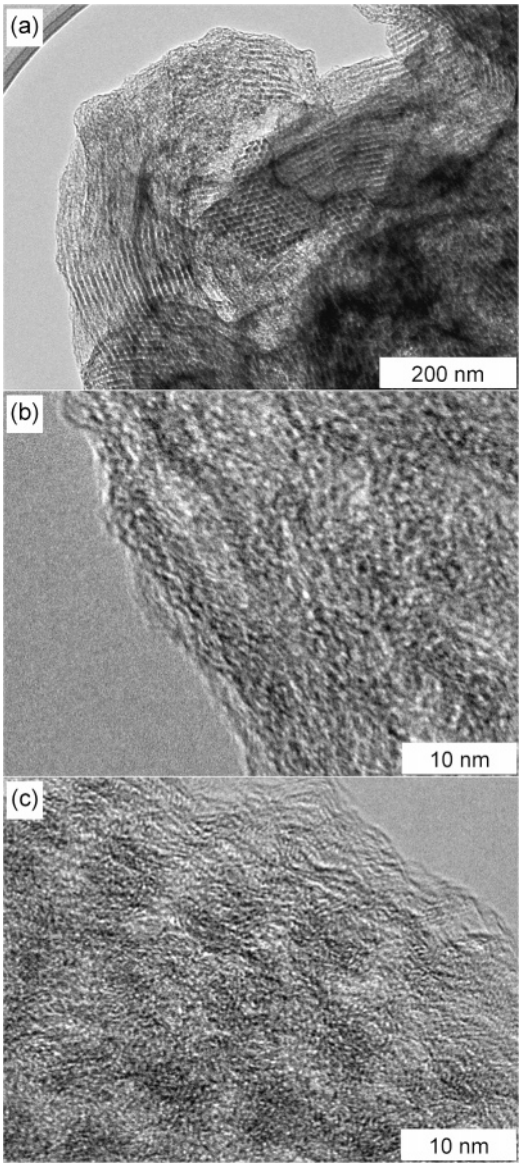

Figure 3. TEM images of the nanocasted OMC replica of SBA-15.

The microstructure the OMC replica was also investigated. The wide-angle XRD of the OMC (inset in Figure 2a) contains two broad and weak signals at 26° and 45°, corresponding to (002) and a superposition of the (100) and (101) reflections of the graphite structure. It suggests that the material possesses some graphitic nature. TEM images of the OMC replica (Figure 3) further reveal the ordered pore arrangement and the microstructure of the material. The hexagonal arrangement of carbon rods is clearly observed in Figure 3a. The carbon rods are 7.0 nm in diameter, and the inter-rod spacing is about 2.9 nm. In addition, high-resolution images (Figure 3b and c) show that these carbon rods consist of graphene layers and fragments that are roughly parallel to the rod axis. The structure is quite unique as compared with the CMK-3 material prepared from sucrose[5b] that mainly consists of graphene layers packed in a disordered fashion,[5e] or with the CMK-3G material with mesophase pitches morphology.[9] The distinct microstructure of the OMC replica from Ppy may be related to the packing

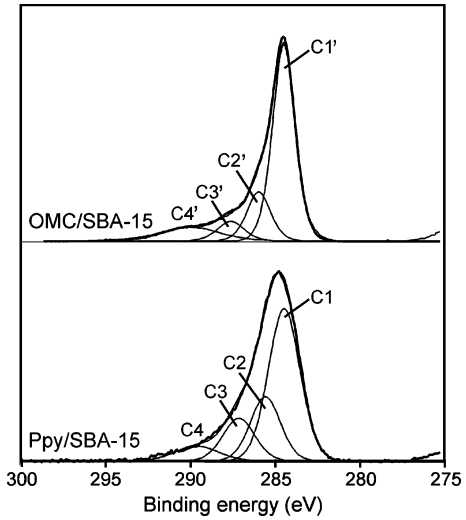

Figure 4. XPS spectra of Ppy/SBA-15 and OMC/SBA-15 composites. The deconvolution results are also included.

of linear polymer Ppy and its pyrolysis behavior with the existence of iron in the pores of SBA-15.

XPS spectroscopy was also applied to characterize the nature of the carbon species in Ppy/SBA-15 and OMC/SBA-15 composites. The spectra of the C 1s regions and their deconvolution results are shown in Figure 4. For Ppy/SBA-15 composite, the binding energy of the C 1s group can be deconvoluted to four different species, attributed to the carbon atoms in the neutral pyrrole rings (C1 and C2) and the carbons (C3 and C4) directly bonded to the positively charged nitrogens that are oxidized and are the charge carriers of the conducting polymer.[13] The ratio of the carbons in the neutral pyrrole rings (C1 and C2, 78 at. % in total) to those bonded to the positively charged nitrogen (C3 and C4, 22 at. % in total) is very close to that of the bulk Ppy material without reoxidized species.[13]

On the other hand, the C 1s spectrum of the OMC/SBA-15 composite consists of a sharp peak at 284.3 eV (C1′) which is assigned to the graphitic carbon species. The full width at half-maximum (fwhm) is 1.5 eV, a value larger than those for the related CMK-type carbon materials pyrolyzed at the similar temperature.[14] This suggests a relatively disordered packing of graphene layers in the OMC/SBA-15 composite, which is in line with results of XRD and TEM investigations. The small peak at 290.2 eV (C4′) is attributed to the plasmon peak and to some contribution of the so-called shake-up satellite due to $\pi \rightarrow \pi^*$ transitions.[13d] In addition, there are two peaks (19 at. % in total) assigned to oxidized carbon species (C2′ and C3′). They might be carbon atoms connected to the residual nitrogen atoms, or those on the edge of graphene layers that are oxidized in air. The pure OMC material obtained after the removal of the silica host and the iron showed the same C 1s XPS spectrum as in the OMC/SBA-15 composite. The quantitative analysis reveals that the material contains about 5.5 at. % of nitrogen, less than 1 at. % iron, and nearly no silicon. It should be mentioned that the almost complete removal of iron by HCl solution suggests that iron species produced during the pyrolysis of Ppy are fully accessible to the acid and are not embedded or coated with carbon that would protect them from dissolution.

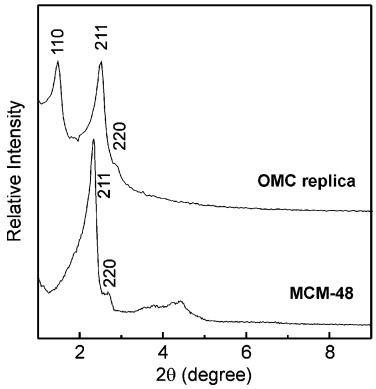

Figure 5. XRD patterns of MCM-48 and its OMC replica.

The synthetic route was also used to prepare OMC replica of MCM-48 with cubic *Ia*3*d* structure.[15] Figure 5 shows XRD patterns of the host MCM-48 and its OMC replica (prepared from the host MCM-48 impregnated with 1.0 g of $FeCl_3$ per g of MCM-48). The parent MCM-48 shows highly ordered cubic *Ia*3*d* structure, as indicated by the well-resolved (211), (220), and higher-order reflections. The XRD pattern of its OMC replica also contains intense and well-resolved reflections. The additional peak appearing at 2θ below 2° indicates a decrease in symmetry of the material, which has also been observed for OMC replica of MCM-48 from sucrose (CMK-1) with cubic $I4_132$ structure.[5a] The reason for such a transformation may be due to the displacement of two noninterconnecting networks of pyrolyzed carbon in the host MCM-48 after dissolution of host silica.[5a] Therefore, the XRD pattern suggests that the as-prepared OMC replica also transforms its structure to cubic $I4_132$ structure during the removal of MCM-48 silica.

Conclusions

In summary, a new route for facile template synthesis of OMC materials using Ppy as carbon precursor has been described. The stoichiometric vapor-phase oxidative polymerization of Ppy at room-temperature ensures a rational control of carbon loading. The as-made materials have large surface area and pore volume. The OMC replicas also have unique carbon microstructures with some graphitic nature. In principle, the synthesis method is applicable for mesoporous silica hosts with different morphologies even of high aspect ratio. Our preliminary results of research along these lines indicate that OMC replicas with macroscopic fiber morphology can be prepared by using mesoporous silica fibers as the template.

CM049164V